J IRAN CHEM SOC (2016) 13:7–18
DOI 10.1007/s13738-015-0706-9

ORIGINAL PAPER

Direct synthesis of benzo[*a*]carbazoles by palladium-catalyzed domino reactions: synthesis and photophysical properties of diverse benzo[*a*]carbazoles

Mohammad Ghanbari[1] · Ebrahim Kianmehr[2] · Sara Karimi Behzad[3] · Seik Weng Ng[4,5]

Received: 4 January 2015 / Accepted: 16 July 2015 / Published online: 31 July 2015

Abstract A direct, concise, and atom-economical synthetic method for the generation of benzo[*a*]carbazoles, using a palladium-catalyzed reaction has been developed. The reaction produces gave various benzo[*a*]carbazoles in good to excellent yields, through Knoevenagel condensation followed by intramolecular ortho-arylation. The synthetically attractive feature of the procedure is reflected by its applicability to a wide range of indole and bromobenzaldehyde derivatives. Mechanistic aspects of the reaction involves the formation of a single isomer of two possible products which leads to the formation of benzo[*a*]carbazoles via a palladium-catalyzed C–H bond functionalization reaction. The development of the annulation reaction with a wide substrate scope provided a unique opportunity to evaluate photophysical properties of a series of benzo[*a*]carbazoles. Almost all the compounds evaluated in this study were found to emit purple to blue light in the visible region. Some interesting structure–property correlations are also described.

Keywords Homogeneous catalysis · C–C coupling · Palladium · Photophysical properties · Quantum yield

Introduction

Aryl- and heteroaryl-annulated carbazoles play an essential role in various areas of synthetic and medicinal chemistry that have been comprehensively reviewed [1–3], they are particularly noted for their diverse biological and pharmacological activities [4–13]. They are classified into [*a*], [*b*] and [*c*]-types based on the position at which the aryl ring is fused to the carbazole nucleus (Fig. 1). In the case of heteroaryl derivatives, each positional isomer is further sorted according to the mode of annulation, as exemplified by heteroaryl-[2,3-*a*] and -[3,2-*a*]carbazoles.

Among these derivatives, a number of biologically active compounds possess a benzo[*a*]carbazole framework. According to their substituents, these compounds can exhibit antifungal and antitumor activities [11, 14], antiestrogenic properties [15], or kinase inhibitory activities [16]. A series of simple benzo[*a*]carbazoles, e.g., **1**, have been shown agonists of the human thrombopoietin receptor [6]. Other benzo[*a*]carbazoles, such as **2** and **3**, exhibit a pronounced antitumor activity against leukemia, renal tumor, colon cancer, and malignant melanoma tumor cell lines (Fig. 2) [7].

On the other hand, recently applications of aryl- and heteroaryl-annulated carbazoles have been increasing in the field of organic electronics. In this regard, benzo[*a*] and indolo[3,2-*b*]carbazole derivatives have been utilized as

Electronic supplementary material The online version of this article (doi:10.1007/s13738-015-0706-9) contains supplementary material, which is available to authorized users.

✉ Mohammad Ghanbari
ghanbari-m@kashanu.ac.ir

✉ Ebrahim Kianmehr
kianmehr@khayam.ut.ac.ir

[1] Department of Organic Chemistry, Faculty of Chemistry, University of Kashan, Kashan, Iran

[2] School of Chemistry, College of Science, University of Tehran, 1417614411 Tehran, Iran

[3] Department of Chemistry, Shahid Beheshti University, G.C, 1983963113 Tehran, Iran

[4] Department of Chemistry, University of Malaya, 50603 Kuala Lumpur, Malaysia

[5] Chemistry Department, Faculty of Science, King Abdulaziz University, PO Box 80203, Jeddah, Saudi Arabia

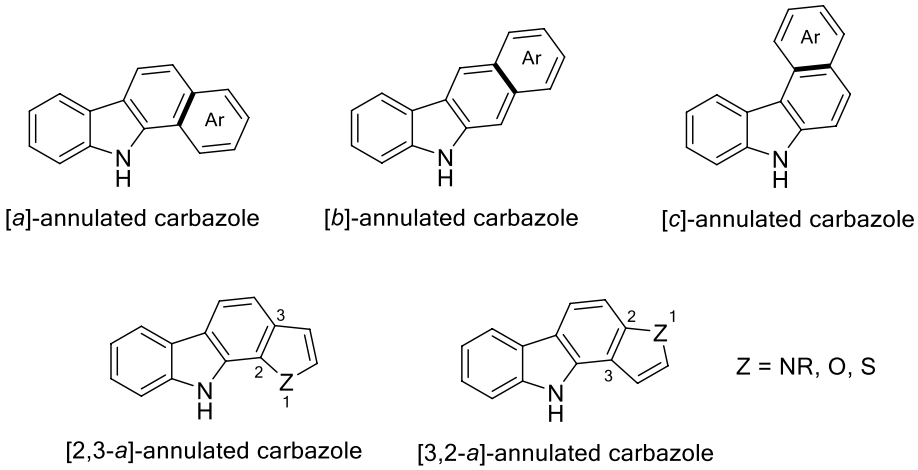

Fig. 1 Classification of aryl- and heteroaryl-annulated carbazoles

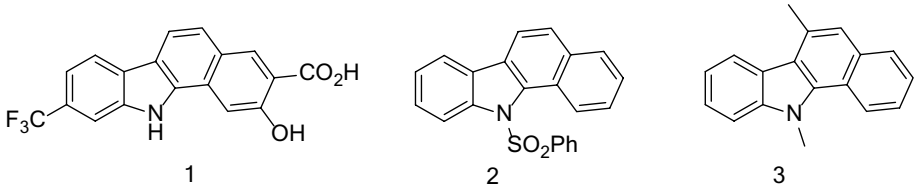

Fig. 2 Bioactive compounds with a benzo[*a*]carbazole core structure

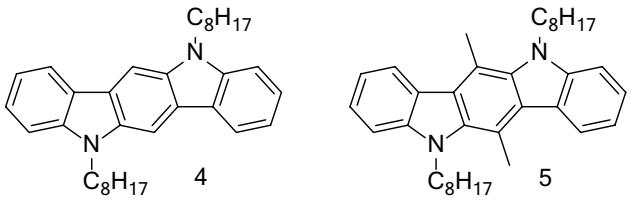

Fig. 3 Electroactive compounds with an Indolocarbazole core structure

molecular platforms for luminescent, host materials and hole-transporting materials in OLEDs (**4** in Fig. 3) [17–23]. Furthermore, Indolo-[3,2-*b*]carbazoles **5** represent high-performance *p*-channel semiconductors with good environmental stability for organic electronic applications (Fig. 3) [24–26].

Also, optical, electrochemical, magnetic, and conductive properties of polyindolocarbazoles and polydiindolocarbazoles with incorporation of indolo[3,2-*b*]carbazoles into a polymer chain have been investigated [27]. It is clear, aryl- and heteroaryl-annulated carbazoles play a fundamental role in a variety of aspects, but a major interest as electroactive and photoactive materials has been poured into indolo[3,2-*b*]carbazole frameworks perhaps due to the structural accessibility. Therefore, development of straightforward synthetic methods for other aryl- and heteroaryl-annulated carbazoles like benzo[*a*]carbazoles surely opens up a further opportunity to utilize benzo[*a*]carbazoles as material sources. Unsurprisingly, many efforts have been made to develop methodologies, ranging from thermal and photochemical cyclization, palladium-catalyzed cross-coupling reactions, Fischer indolization, Diels–Alder reactions, gold-catalyzed intramolecular cyclization reactions, and irradiation of a benzotriazole derivative, for the synthesis of benzo[*a*]carbazole derivatives [1, 28–34]. In 1993, Hill et al. reported the synthesis of the benzo[*a*]carbazole derivatives using a palladium-mediated oxidative cyclization as the key step. In last step, oxidative cyclization of intermediate with palladium(II) acetate provided 5,6-maleimido-11*H*-benzo[*a*]carbazole in 14 % yield [35]. A few years later, De Koning and co-workers have described the synthesis of the 11*H*-benzo-[*a*]carbazoles from 2-bromoindole-3-carbaldehyde using the base-induced photocyclization of the 2-arylindoles as the key step. A palladium-catalyzed Suzuki cross-coupling of intermediate with the boronic acids afforded the corresponding 2-arylindoles, which were transformed to the 11*H*-benzo[*a*]carbazoles via a base-induced photocyclization [36]. In 2009, Jiao et al. demonstrated the first palladium-catalyzed cycloaromatization of 2- and 3-arylindoles with internal alkynes through dual activation of C–H bonds. The reaction outcomes provide a new strategy for constructing aromatic compounds from biaryls and internal alkynes [37]. One year later, Fujii and co-workers have developed a novel gold-catalyzed intramolecular cascade cyclization for the synthesis of aryl- and heteroaryl-annulated[*a*]carbazoles. The reaction is applicable to various aryl-annulated[*a*]carbazoles containing an alkyl or aryl substituent [38]. Combined

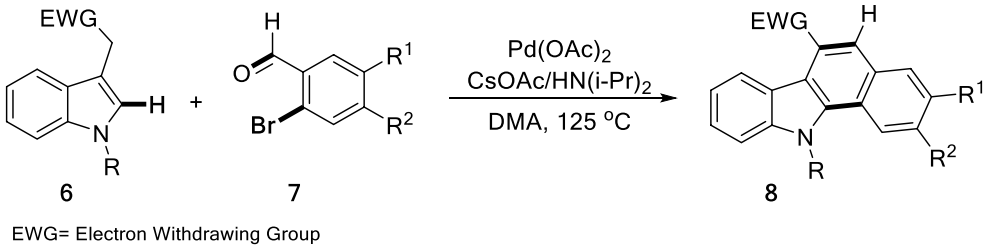

Scheme 1 Synthesis of benzo[*a*]carbazoles: our strategy

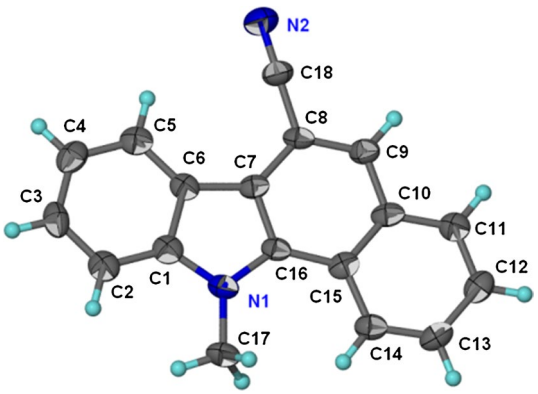

Fig. 4 Solid-state molecular structure of **8a**

directed ortho and remote metalation-cross-coupling of 3-(diethylcarbamoyl)1-methyl-1*H*-indol-2-ylboronic acid reported by Victor Snieckus and co-workers is another approach for synthesis of benzo[*a*]carbazoles and their derivatives [39]. Recently, Zhang and co-workers have synthesized benzo[*a*]carbazoles and indolo[2,3-*a*]- carbazoles via photoinduced carbene-mediated C–H insertion reaction. With structurally *o*-toluidine as the starting material, this synthetic strategy can provide benzo[*a*]carbazoles and their derivatives in 6 or 7 steps [40]. Despite these numerous studies, most of these procedures have involved several steps, and the overall yields were, in general, not very good. Moreover, the starting materials were often not readily available. The development of a direct, concise, and atom-economical synthetic route to this class of compounds, producing minimum waste/byproduct, would therefore be of considerable interest for drug discovery and material chemistry. In modern organic chemistry, both tandem reactions and C–H functionalization are considered as efficient tools for the synthesis of complex molecules in terms of atom economy. As part of our ongoing research program on the development of efficient methods in organic synthesis and on the preparation of heterocyclic compounds [41–46], to develop a more atom economical and direct

Table 1 Crystal data and refinement details for compound **8a**

Molecular formula	$C_{18}H_{12}N_2$
Formula weight	256.30
Crystal size (mm^3)	1.06 × 0.47 × 0.62
Crystal color	Yellow
Wavelength (Å)	1.54184
Crystal system	Orthorhombic
Space group	$P2_12_12_1$
a (Å)	4.4152 (1)
b (Å)	16.2537 (5)
c (Å)	17.7377 (5)
α (°)	90
β (°)	90
γ (°)	90
V ($Å^3$)	1272.92 (6)
Z	4
F (000)	536.0
Calculated density (g/cm^3)	1.337
μ (mm^{-1})	0.620
T (*K*)	100
Final *R* indices	$R = 0.0625$, $wR^2 = 0.1651$
S	1.057

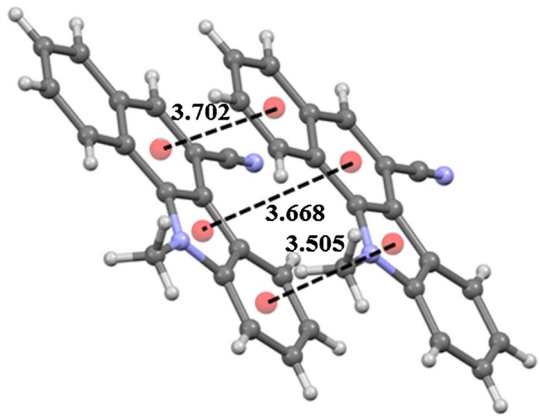

Fig. 5 The *π*–*π* interactions in prepared compound **8a**

Table 2 Synthesis of benzo[*a*] carbazoles by palladium-catalyzed reactions

Entry	Indole	Benzaldehyde	Product	Yield
1	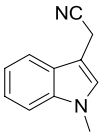 **6a**	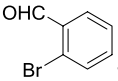 **7a**	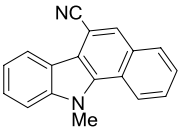 **8a**	**89%**
2	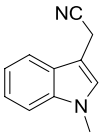 **6a**	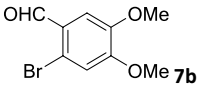 **7b**	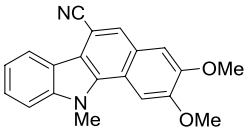 **8b**	**91%**
3	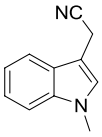 **6a**	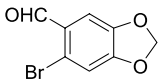 **7c**	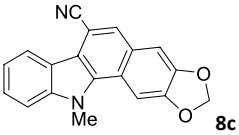 **8c**	**90%**
4	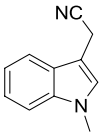 **6a**	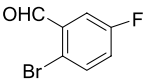 **7d**	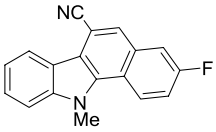 **8d**	**79%**
5	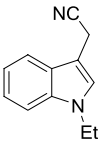 **6b**	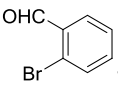 **7a**	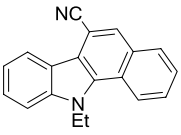 **8e**	**87%**
6	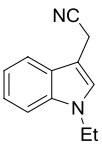 **6b**	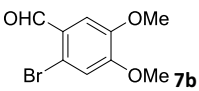 **7b**	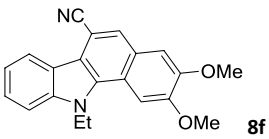 **8f**	**91%**
7	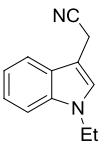 **6b**	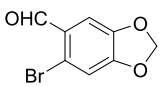 **7c**	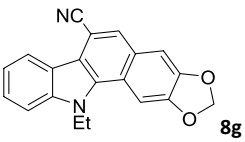 **8g**	**89%**
8	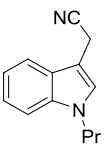 **6c**	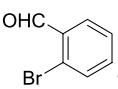 **7a**	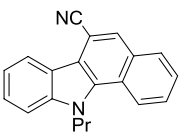 **8h**	**86%**
9	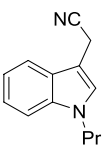 **6c**	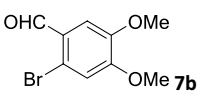 **7b**	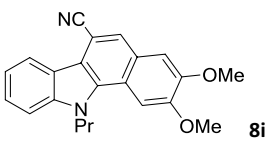 **8i**	**89%**
10	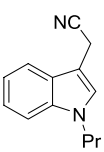 **6c**	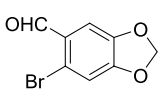 **7c**	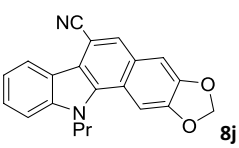 **8j**	**86%**
11	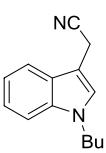 **6d**	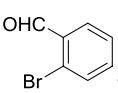 **7a**	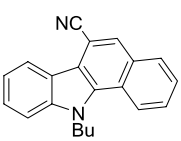 **8k**	**84%**

Table 2 continued

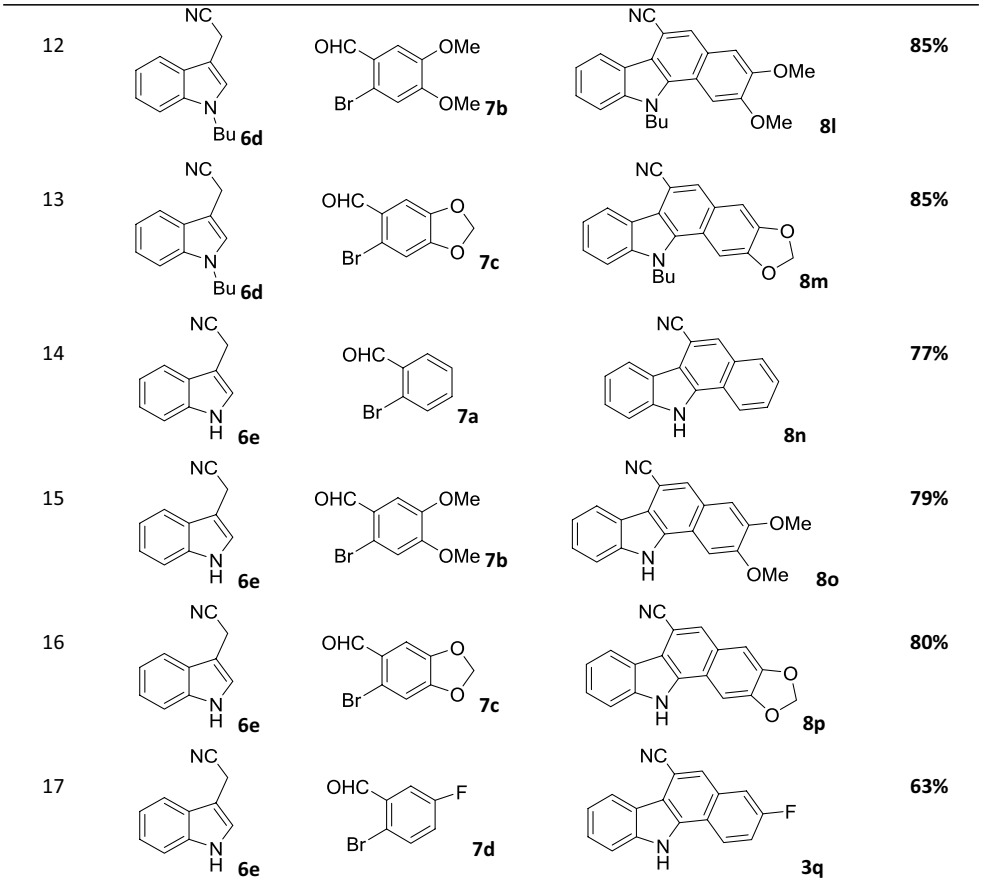

Standard reaction conditions: **6** (1 mmol), **7** (1.6 equiv.), $Pd(OAc)_2$ (10 mol %), CsOAc (3 equiv.), $HN(i\text{-}Pr)_2$ (1 equiv.), DMA (3 mL), 125 °C, 36 h, Ar. Yields are given for the isolated products

synthetic method to benzo[*a*]carbazoles, we designed a direct palladium-catalyzed route for the synthesis of novel benzo[*a*]carbazoles through sequential C–C bond formation and C–H bond functionalization in one-pot by using readily available starting materials [47]. We now report full details of our study on the synthesis of benzo[*a*]carbazoles based on a preliminary communication. The overview of our strategy is summarized in Scheme 1. With the broad diversity of benzo[*a*]carbazole derivatives obtained under the standard reaction conditions, gave us an opportunity to understand the effect of frameworks and substituents on the optical properties of benzo[*a*]carbazoles.

Results and discussion

Synthesis of Benzo[*a*]carbazoles Derivatives

Our preliminary investigation revealed that the best conditions for the formation of 11-methyl-11*H*-benzo[*a*]carbazole-6-carbonitrile **8a** involved the use of 1 equiv. (1-methyl-1*H*-indol-3-yl)acetonitrile **6a** and 1.6 equiv. 2-bromobenzaldehyde **7a** in the presence of cesium acetate (CsOAc, 3 equiv.), diisopropylamine ($HN(i\text{-}Pr)_2$, 1 equiv.) and 10 mol% $Pd(OAc)_2$ in *N*,*N*-dimethylacetamide (DMA, 3 mL) at 125 °C for 36 h under an argon atmosphere. This led to the formation of **8a** in 89 % yield by a route in which both inter- and intramolecular carbon–carbon bond-forming reactions took place in one step. The structure of **8a** was characterized by spectroscopic analysis and the constitution of the product could be unambiguously assigned by X-ray crystal structure analysis (Fig. 4) [48].

Crystal data, refinement details, and selected bond distances and angles for the title compound **8a** are listed in Table 1 and Table S1 (electronic supplementary material), respectively. Compound **8a** is crystallized in the $P2_12_12_1$ space group of the Orthorhombic system. The connections between the layers in the ab plane are face-to-face π–π type stacking interactions between pyrrole and phenyl, phenyl and phenyl rings of two adjacent molecules of **8a** with a centroid–centroid distance of 3.50, 3.66, and 3.70 Å (Fig. 5).

To delineate this approach, particularly with regard to construction of a library of compounds, the optimized

Table 3 Synthesis of benzo[*a*] carbazole derivatives

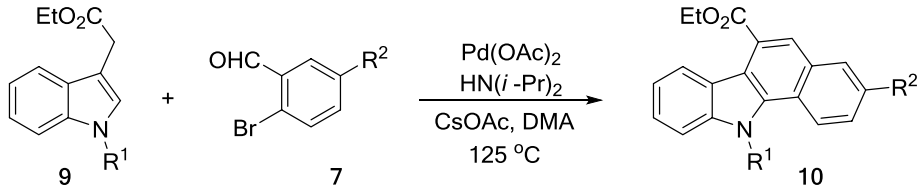

Entry	Indole	Benzaldehyde	Product	Yield
1	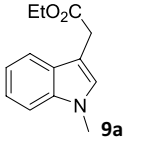 **9a**	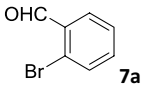 **7a**	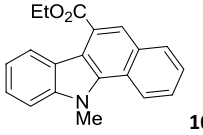 **10a**	**81%**
2	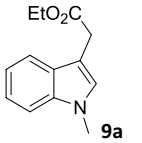 **9a**	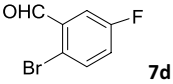 **7d**	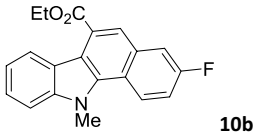 **10b**	**76%**
3	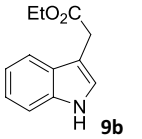 **9b**	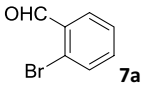 **7a**	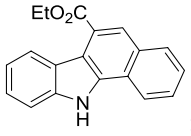 **10c**	**61%**
4	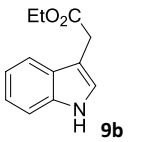 **9b**	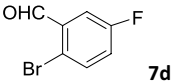 **7d**	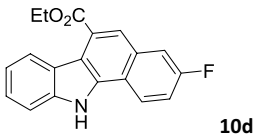 **10d**	**57%**

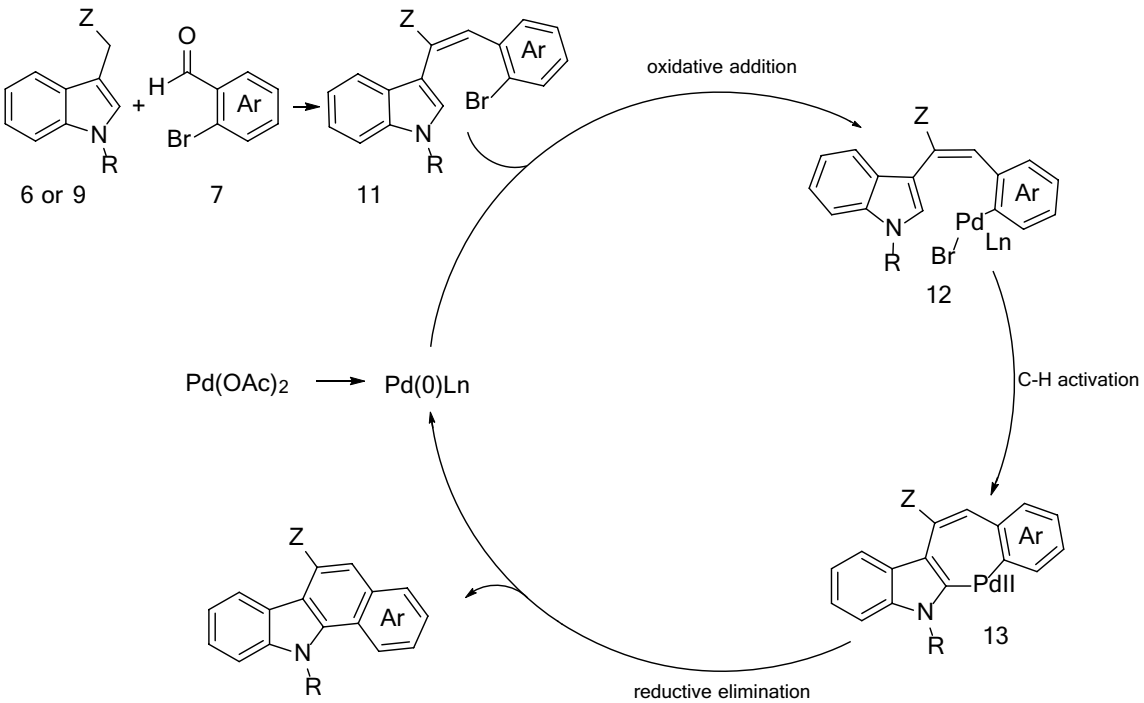

Scheme 2 Proposed mechanism for the formation of the benzo[*a*]carbazole ring

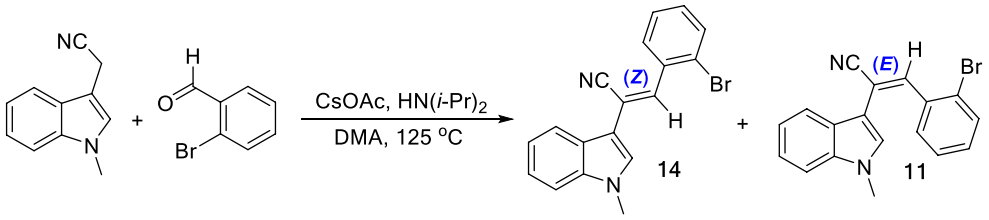

Scheme 3 Two possible products in the Knoevenagel condensation reaction

reaction conditions were applied to the synthesis of various benzo[*a*]-carbazoles. The results are summarized in Table 2. Besides **7a**, 2-bromobenzaldehyde derivatives such as **7b**–**7d** having a methoxy, dioxole or fluor group on the phenyl group underwent the palladium-catalyzed cyclization with (1-methyl-1*H*-indol-3-yl)acetonitrile (**6a**) to give the corresponding benzo[*a*]-carbazole (**8b**–**8d**) in good to excellent yields (Table 2, entries 1–4). *N*-Alkylindoles **6b**–**6d** bearing an ethyl, propyl or butyl group on the nitrogen atom also reacted with **7a**–**7c** to afford desired **8** (Table 2, entries 5–13). We also investigated the reaction of 2-(1*H*-indol-3-yl)acetonitrile **6e** containing free NH group

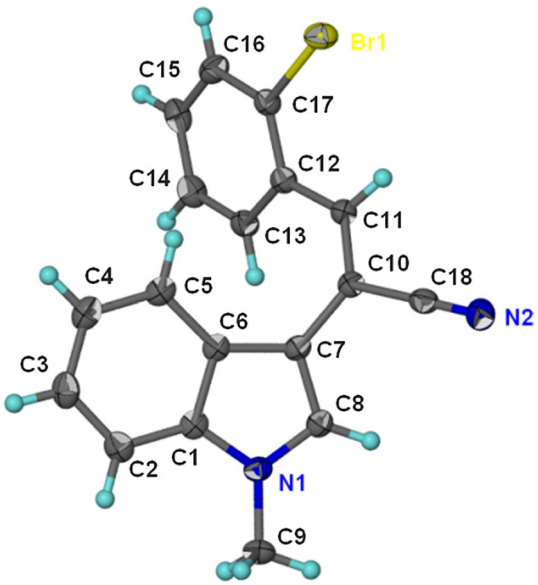

Fig. 6 Solid-state molecular structure of *E* isomer **11**

(Table 2, entry 14). In this case, a comparable clean reaction was observed and 11*H*-benzo[*a*]carbazole-6-carbonitrile **8n** was synthesized in one-pot by a domino reaction in good yield. Remarkably, the palladium-catalyzed annulation provides **8n** in only one step from commercially available **6e** and **7a**, in contrast to the multi-step synthetic route reported earlier [8]. Synthetically, it is very useful that free NH indole does not change the reaction pathway, and satisfactory yields of **8** were obtained using these free NH indoles (Table 2, **8n**–**8q**).

To further explore the potential of this methodology for the synthesis of benzo[*a*]carbazole derivatives, we investigated the reaction with another indole backbone. We found that the benzo[*a*]carbazole synthesis protocol is also compatible with ethyl(1-alkyl-1*H*-indol-3-yl)acetate **9**, being transformed into corresponding benzo[*a*]carbazole derivatives **10** (Table 3).

Ethyl 2-(1-methyl-1*H*-indol-3-yl)acetate **9a** thus reacted with 2-bromobenzaldehyde **7a** to give ethyl 11-methyl-11*H*-benzo[*a*]carbazole-6-carboxylate **10a** as the sole product. Besides **7a**, 2-bromo-5-fluorobenzaldehyde **7d** having a fluor group on the phenyl group underwent the palladium-catalyzed cyclization with ethyl 2-(1-methyl-1*H*-indol-3-yl)acetate **9a** to give the corresponding benzo[*a*]-carbazole **10b** in good yield (Table 3, entries 2). Ethyl 11*H*-benzo[*a*]carbazole-6-carboxylate **10c** was produced in 61 % yield by the cyclization reaction between ethyl 2-(1*H*-indol-3-yl)acetate **9b** and 2-bromobenzaldehyde **7a**. The reaction of ethyl 2-(1*H*-indol-3-yl)acetate **9b** with 2-bromo-5-fluorobenzaldehyde **7d** also proceeded to give the corresponding benzo[*a*]-carbazole **10d** in moderate yield (Table 3, entriy 4). Remarkably, our procedure can be applied for

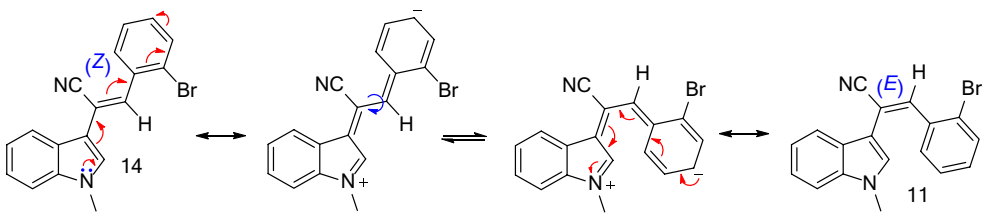

Scheme 4 Plausible interconversion of *Z* and *E* isomers

the synthesis of a variety of benzocarbazoles with different functional groups by using other indole backbones or different halobenzaldehydes in only one step from commercially available starting materials [49], in contrast to the multi-step procedures reported in literature. It should be noted that this reaction is also applicable with free NH indoles than most of previously reported procedure [1, 8].

Reaction Mechanism

The mechanism of the reaction has not been established experimentally; however, on the basis of previous chemistry [50–52], a plausible mechanism for the synthesis of the benzo[*a*]carbazole ring system via Knoevenagel condensation followed by intramolecular ortho-arylation is described in Scheme 2. According to the proposed mechanism, intermediate **11** is formed by the Base-induced Knoevenagel condensation reaction between **6** (or **9**) and **7**. The first step of the catalytic cycle involves formation of aryl–palladium(II) intermediate **12** by the oxidative addition of C–Br bond to the Pd^0 species. Then, intramolecular ortho-arylation to the adjacent aryl C–H bond gives the seven-membered palladacycle intermediate **13**, which reductively eliminates to the desired product with the regenerating the Pd(0) catalyst. To confirm the proposed mechanism, we studied the mechanistic pathway of the reaction. The reaction of **6a** with **7a** was investigated in the absence of $Pd(OAc)_2$, where we isolated the Knoevenagel condensation intermediate after eight hours (Scheme 3). There are two possible products for the Knoevenagel condensation intermediate, (*Z*)-3-(2-bromophenyl)-2-(1-methyl-1*H*-indol-3-yl)acrylonitrile **14** and (*E*)-3-(2-bromophenyl)-2-(1-methyl-1*H*-indol-3-yl) acrylonitrile **11**.

However, it is anticipated that the both isomers are formed in the Knoevenagel condensation reaction but to our surprise only the *E* isomer was obtained in 86 % yield under the reaction conditions which was confirmed by NMR analysis of the crude product and X-ray crystallography data (Please see the electronic supplementary material) (Fig. 6) [53].

Z and *E* interconversion to the more stable isomer, probably *E* under conditions reaction, may be facilitated by resonance in the conjugated system (Scheme 4) [54].

Crystal data, refinement details, and selected bond distances and angles for the title compound **11** are listed in Tables 4 and Tables S2 (electronic supplementary material), respectively. Compound **11** is crystallized in the $P2_1/c$ space group of the monoclinic system. The connections between the layers in the ab plane are face-to-face C–H-π interaction between C–H of methyl group and phenyl rings of two adjacent molecules of **11** with distance of 2.69 Å (Table 5; Fig. 7).

Table 4 Crystal data and refinement details for compound **11**

Molecular formula	$C_{18}\,H_{13}\,Br_1\,N_2$
Formula weight	337.20
Color	Yellow
Crystal size (mm^3)	0.21 × 0.65 × 0.35
Crystal color	Yellow
Wavelength (Å)	1.54184
Crystal system	Monoclinic
Space group	$P2_1/c$
a (Å)	7.5332(1)
b (Å)	7.5653(1)
c (Å)	25.3155(3)
α (°)	90
β (°)	93.932(1)
γ (°)	90
V ($Å^3$)	1439.36(3)
Z	4
F (000)	680
Calculated density. (g/cm^3)	1.556
μ (mm^{-1})	3.827
T (*K*)	100
Final *R* indices	$R = 0.0299$, $wR^2 = 0.0868$
S	1.064

Table 5 Significant intermolecular interactions [interatomic distance (Å) and bond angels (°)] for **11**

D–H···A	D–H	H…A	D···A	D–H···A
C(5)–H(5)···Br(1)$^{\#1}$	0.95	2.89	3.415(2)	116
C(9)–H(9A)···N(2)$^{\#2}$	0.98	2.56	3.479(3)	156
C(11)–H(11)···Br(1)	0.95	2.73	3.156(2)	108

Symmetry codes: #1: −x,−1/2 + y,1/2 − z; #2: −x, 2 − y, 1 − z

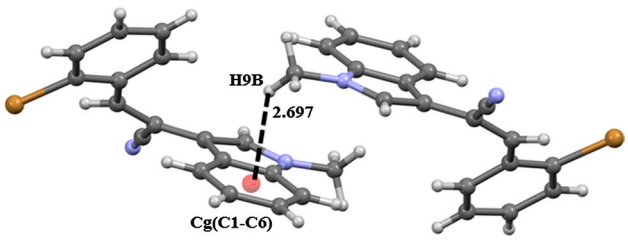

Fig. 7 A perspective view of C–H–*π* interaction in compound **11**

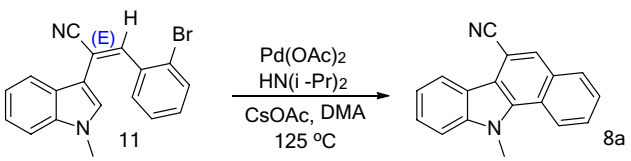

Scheme 5 Formation of the desired product from intermediate **11**

Table 6 Photophysical properties of benzo[*a*]carbazoles

Benzo[*a*]carbazoles	UV–Vis	Emission[a]		Benzo[*a*]carbazoles	UV–Vis	Emission[a]	
	λ_{max} nm (log ε)	λ_{max} nm	Φ^b		λ_{max} nm (log ε)	λ_{max} nm	Φ^b
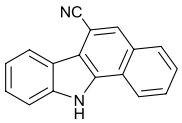 **8n**	250 (4.31), 286 (4.33), 352 (3.48), 371 (3.65)	388, 403	0.199	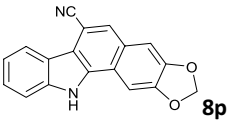 **8p**	273 (3.55), 293 (3.82), 347 (2.92), 365 (2.84)	396	0.193
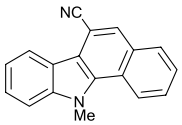 **8a**	247 (4.64), 291 (4.67), 362 (3.88), 382 (4.04)	396, 411	0.298	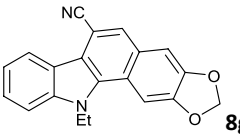 **8g**	262 (4.07), 297 (4.44), 357 (3.49), 377 (3.48)	388, 406, 432	0.373
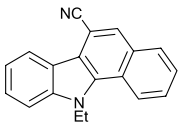 **8e**	250 (4.10), 295 (4.38), 359 (3.41), 378 (3.54)	394, 412	0.308	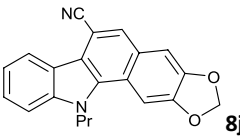 **8j**	241 (4.46), 293 (4.59), 348 (3.80), 372 (3.66)	389, 407	0.244
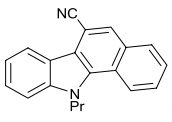 **8h**	265 (3.91), 296 (4.22), 359 (3.27), 378 (3.35)	407, 420	0.296	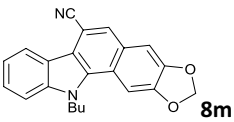 **8m**	245 (4.00), 298 (4.23), 360 (3.37), 379 (3.37)	388, 406	0.059
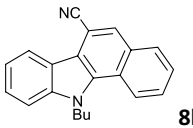 **8k**	241 (4.53), 288 (4.45), 358 (3.76), 375 (3.84)	396, 412	0.198	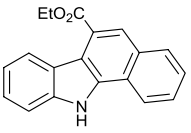 **10c**	254 (4.50), 288 (4.57), 308 (4.19), 370 (3.77)	415	0.177
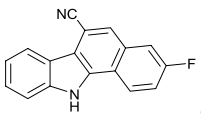 **8q**	252 (4.58), 288 (4.69), 362 (3.85), 378 (3.99)	399, 414	0.271	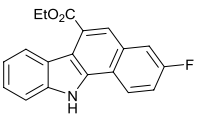 **10d**	254 (4.71), 290 (4.82), 309 (4.38), 374 (4.01)	423	0.133
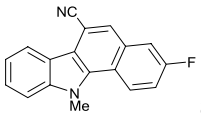 **8d**	244 (4.63), 290 (4.66), 366 (3.82), 386 (4.03)	405, 420	0.283	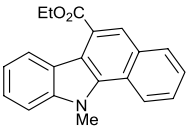 **10a**	246 (4.64), 290 (4.61), 210 (4.24), 376 (3.83)	424	0.263
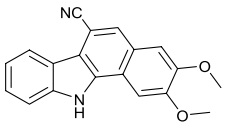 **8o**	291 (4.61), 330 (3.93), 345 (3.82), 366 (3.75)	388, 398	0.234	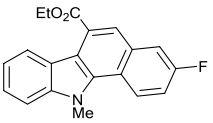 **10b**	244 (4.80), 292 (4.80), 312 (4.36), 380 (4.01)	433	0.173
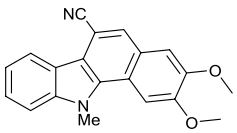 **8b**	250 (4.32), 295 (4.04), 310 (3.85), 378 (3.47)	389, 406	0.267				

Dichloromethane was used as a solvent for measurement of UV–Vis ($c = 1.5 \times 10^{-5}$ M) and fluorescence ($c = 1.5 \times 10^{-6}$ M) spectra

[a] Excited at 360 nm

[b] Determined with reference to the quantum yield of Quinine sulfate

The proposed mechanism was confirmed by subjecting intermediate **11** to the reaction conditions, which led to the formation of the desired product (Scheme 5). The reaction did not go to completion and we obtained **8a** in only 77 % yield.

Photophysical properties of benzo[*a*]carbazole

With the broad diversity of benzo[*a*]carbazole derivatives obtained under the standard reaction conditions, we

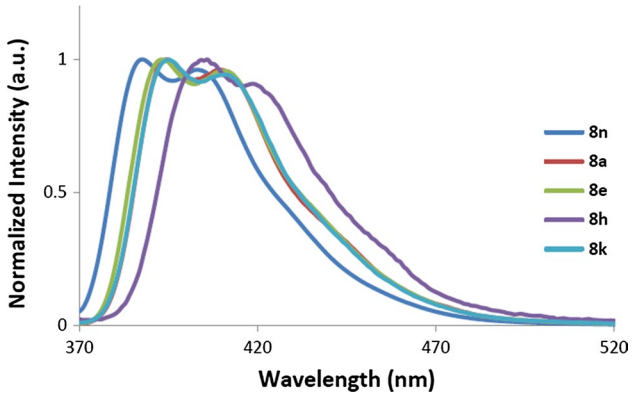

Fig. 8 Comparison emission spectrum of *N*-alkyl derives in CH_2Cl_2 ($c = 1.5 \times 10^{-6}$ M), excited at 360 nm

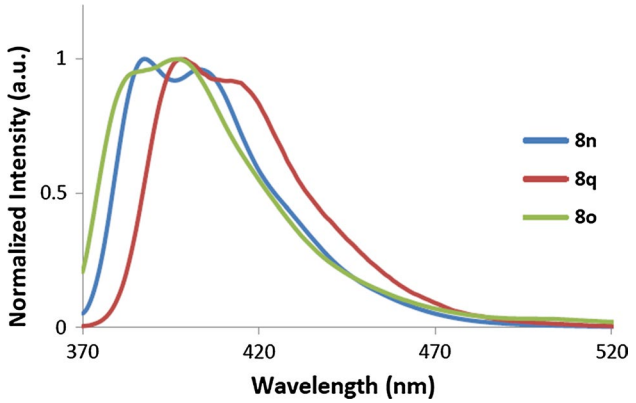

Fig. 9 Emission spectrum of **8n**, **8q** and **8o** in CH_2Cl_2 ($c = 1.5 \times 10^{-6}$ M), excited at 360 nm

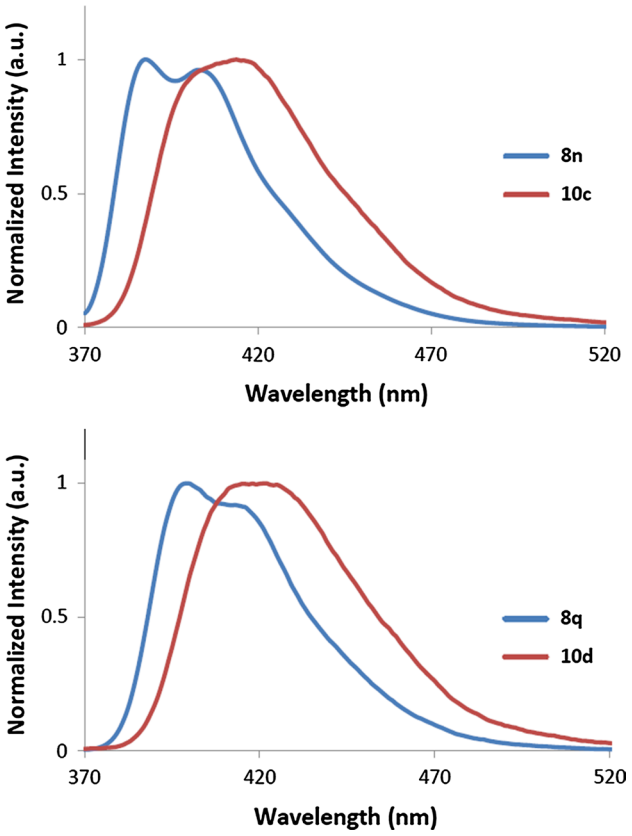

Fig. 10 Comparison emission spectrum of **8n** with **10c** and **8q** with **10d** in CH_2Cl_2 ($c = 1.5 \times 10^{-6}$ M), excited at 360 nm

became intensely interested in the potential of the products as electroactive materials and the photophysical properties of the benzo[*a*]carbazoles was investigated; the results are collected in Table 6. Quantum yields were determined by the comparative method described by Williams et al. [55] and the results were obtained according to Eq. (1):

$$\Phi_X = \Phi_{ST}\left(\frac{Grad_X}{Grad_{ST}}\right)\left(\frac{\eta_X^2}{\eta_{ST}^2}\right) \quad (1)$$

where the subscripts ST and X denote standard and test respectively, Φ is the Quantum yield, *Grad* the gradient from the plot of integrated emission intensity *vs.* absorbance, and η the refractive index of the solvent. Quantum yields were measured with Quinine sulfate ($\Phi = 0.54$ in 0.1 M H_2SO_4) as the Ref. [56]. First, we focused on evaluating the effect of substituents on benzo[*a*]carbazole core structure. For example, in the UV–Vis spectrum of 11*H*-benzo[*a*]carbazole-6-carbonitrile (**8n**), the absorption bands ascribed to the π–π^* transitions with the relatively large extinction coefficients were detected, ranging from 250 to 371 nm. It was then found that **8n** ($\Phi = 0.199$) exhibits purple emission derived from the emission λ_{max} around 388 and 403 nm.

Although the absorption and emission patterns of **8a**, **8e**, **8h,** and **8k** containing alkyl group on the nitrogen atom of **8n** resemble those of **8n**, the introduction of the alkyl group was always accompanied by a red-shift of the emission spectra (**8n** vs **8a**, **8e**, **8h**, or **8k**, Fig. 8). Moreover, quantum yield of these compounds increased with introduction of alkyl group on the nitrogen atom except for butyl group.

A similar correlation was also observed between the other *N*-alkylbenzo[*a*]carbazole compared with NH free benzo[*a*]carbazole derivative (**8q** vs. **8d, 8o** vs. **8b, 8p** vs. **8 g, 10c** vs. **10a, 10d** vs. **10b,** Please see the electronic supplementary material). Moreover, FL efficiency was found to be highly dependent on the methoxy and fluoro groups, for example, the quantum yield is increased from **8n** (0.199) to **8q** (0.271), and **8o** (0.234). Also, in comparison with **8n**, the methoxy- and fluoro-containing derivatives,**8q** and **8o**, show red-shift and blue-shift, respectively, in the FL spectra (Fig. 9).

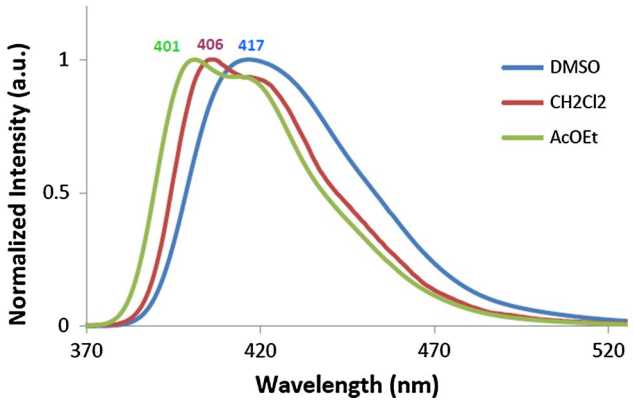

Fig. 11 Solvent-dependent emission spectra of **8d** ($c = 1.5 \times 10^{-6}$ M in each solvent) excited at 360 nm

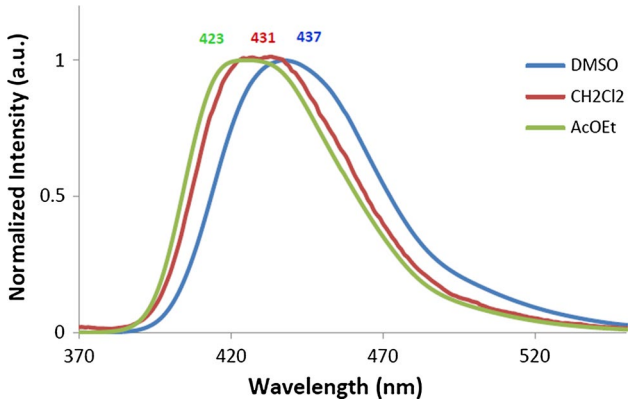

Fig. 12 Solvent-dependent emission spectra of **10b** ($c = 1.5 \times 10^{-6}$ M in each solvent) excited at 360 nm

Furthermore, the functional group change from **8n** (CN) to **10c** (CO_2Et) or **8q** (CN) to **10d** (CO_2Et) resulted in a red-shift of the emission spectra and also a decrease in the quantum yield (Fig. 10).

Next, to gain further insight into the photophysical properties of benzo[*a*]carbazoles, we investigated their spectral dependence on solvent polarity. When benzo[*a*]carbazoles were excited at 360 nm in different solvents, such as ethyl acetate (AcOEt), dichloromethane (CH_2Cl_2), and dimethyl sulfoxide (DMSO), their emission spectra were affected by the solvent polarity. For example, increasing the solvent polarity from EtOAc to DMSO caused a significant positive solvatochromism, with 16 and 14 nm red-shift in the emission spectrums of **8d** and **10b**, respectively (Figs. 11, 12). These results clearly show the solvatochromic properties of the benzo[*a*]carbazoles. The considerable red-shift observed in **8d** and **10b** may be mainly due to the charge transfer character of the emission state leading to the significant change in the dipole moment from the ground state to the excited state in polar solvents [57, 58].

Conclusion

In conclusion, we have demonstrated an efficient and simple method that allows the assembly of two readily accessible building blocks, (1-alkyl-1*H*-indol-3-yl)acetonitrile and 2-bromobenzaldehydes, into benzo[*a*]carbazole. The methodology with substrate diversity enables us to synthesize various derivatives of benzo[*a*]carbazole. The achievement of the short step process is attributed to the successive cross-coupling reaction and subsequent pd-catalyzed cyclization. The reaction can be applied for the synthesis of a variety of benzocarbazoles with different functional groups by using other indole backbones such as ethyl (1- alkyl-1*H*-indol-3-yl)acetate **9** or different 2-halobenzaldehydes. The reaction is also applicable with free NH indoles. Photophysical properties of different derivatives of benzo[*a*] carbazole are described. The evaluation of emission spectra of the products showed that almost all the emission bands appear in the visible region (purple to blue) and that quantum yields are highly dependent on the character of the substituents. Some structure–property correlations on benzo[*a*]carbazoles elucidated in the present study are as follows: (1) Introduction of an alkyl group onto the nitrogen atom enhances quantum yield and causes a red-shift in emission spectra. (2) A butyl group on the nitrogen atom causes decrees in quantum yield values. (3) Change the cyano group to the ester group, shows a large bathochromic shift. (4) The title compounds exhibit positive solvatochromic behavior by increasing the solvent polarity.

Acknowledgments We gratefully acknowledge financial support from the Research Council of the University of Tehran and University of Kashan. Professor Seik Weng Ng gratefully acknowledges grant number UM.C/625/1/HIR/247 from University of Malaya. We thank Professor A. Stephen K. Hashmi and Dr. Ben A. Coombs, Organisch-Chemisches Institute, University of Heidelberg, for providing access to instrumental facilities for photophysical properties and some chemicals.

References

1. A.W. Schmidt, K.R. Reddy, H.-J. Knölker, Chem. Rev. **112**, 3193 (2012)
2. H. Nakano, S. Ōmura, J. Antibiot. **62**, 17 (2009)
3. M. Prudhomme, Eur. J. Med. Chem. **38**, 123 (2003)
4. C.M. Cavazos, S.T. Keir, T. Yoshinari, D.D. Bigner, H.S. Friedman, Cancer Chemother. Pharmacol. **48**, 250 (2001)
5. E. Conchon, F. Anizon, B. Aboab, M. Prudhomme, J. Med. Chem. **50**, 4669 (2007)
6. P.B. Alper, T.H. Marsilje, D. Mutnick, W. Lu, A. Chatterjee, M.J. Roberts, Y. He, D.S. Karanewsky, D. Chow, J. Lao Bioorg. Med. Chem. Lett. **18**, 5255 (2008)
7. U. Pindur, T. Lemster, Recent Res. Devel. Org. Bioorg. Chem **1**, 33 (1997)
8. H.-J. Knölker, K.R. Reddy, Chem. Rev. **102**, 4303 (2002)
9. M. Prudhomme, Curr. Med. Chem. Anti Cancer Agents **4**, 509 (2004)

10. S. Oishi, T. Watanabe, J.-i Sawada, A. Asai, H. Ohno, N. Fujii, J. Med. Chem. **53**, 5054 (2010)
11. Y.-Q. Wang, X.-H. Li, Q. He, Y. Chen, Y.-Y. Xie, J. Ding, Z.-H. Miao, C.-H. Yang, Eur. J. Med. Chem. **46**, 5878 (2011)
12. D. Zhu, M. Chen, M. Li, B. Luo, Y. Zhao, P. Huang, S. Xue, R. Rapposelli, R. Pi, S. Wen, Eur. J. Med. Chem. **68**, 81 (2013)
13. C. Saturnino, D. Iacopetta, M.S. Sinicropi, C. Rosano, A. Caruso, A. Caporale, N. Marra, B. Marengo, M.A. Pronzato, O.I. Parisi, Molecules **19**, 9307 (2014)
14. A. Segall, M. Vitale, V. Perez, M. Pizzorno, J. Pharm. Biomed. Anal. **31**, 1021 (2003)
15. E. Von Angerer, J. Prekajac, J. Med. Chem. **29**, 380 (1986)
16. E. Conchon, F. Anizon, B. Aboab, R.M. Golsteyn, S. Léonce, B. Pfeiffer, M. Prudhomme, Biorg. Med. Chem. **16**, 4419 (2008)
17. I.K. Moon, J.-W. Oh, N. Kim, J. Photochem. Photobiol. A Chem. **194**, 351 (2008)
18. N.-X. Hu, S. Xie, Z. Popovic, B. Ong, A.-M. Hor, S. Wang, J. Am. Chem. Soc. **121**, 5097 (1999)
19. H.-P. Zhao, X.-T. Tao, F.-Z. Wang, Y. Ren, X.-Q. Sun, J.-X. Yang, Y.-X. Yan, D.-C. Zou, X. Zhao, M.-H. Jiang, Chem. Phys. Lett. **439**, 132 (2007)
20. Y. Nagase, H. Shirai, M. Kaneko, E. Shirakawa, T. Tsuchimoto, Org. Biomol. Chem. **11**, 1456 (2013)
21. C. Wang, H. Dong, W. Hu, Y. Liu, D. Zhu, Chem. Rev. **112**, 2208 (2012)
22. S. Lengvinaite, J. Grazulevicius, S. Grigalevicius, R. Gu, W. Dehaen, V. Jankauskas, B. Zhang, Z. Xie, Dyes. Pigm. **85**, 183 (2010)
23. M. Kirkus, J. Simokaitiene, J. Grazulevicius, V. Jankauskas, Synth. Met. **160**, 750 (2010)
24. S. Wakim, J. Bouchard, M. Simard, N. Drolet, Y. Tao, M. Leclerc, Chem. Mater. **16**, 4386 (2004)
25. P.-L.T. Boudreault, A.A. Virkar, Z. Bao, M. Leclerc, Org. Electron. **11**, 1649 (2010)
26. Y. Wu, Y. Li, S. Gardner, B.S. Ong, J. Am. Chem. Soc. **127**, 614 (2005)
27. N. Blouin, A. Michaud, S. Wakim, P.L.T. Boudreault, M. Leclerc, B. Vercelli, S. Zecchin, G. Zotti, Macromol. Chem. Phys. **207**, 166 (2006)
28. R. G. Harvey, Polycyclic aromatic hydrocarbons: chemistry and carcinogenicity, CUP Archive1991
29. J.T. Kuethe, K.G. Childers, Adv. Synth. Catal. **350**, 1577 (2008)
30. E. Conchon, F. Anizon, B. Aboab, M. Prudhomme, Synthesis **16**, 2569 (2008)
31. T. Tsuchimoto, H. Matsubayashi, M. Kaneko, E. Shirakawa, Y. Kawakami, Angew. Chem. Int. Ed. **44**, 1336 (2005)
32. F. Dufour, G. Kirsch, Synlett **2006**, 1021 (2006)
33. K. Tanaka, *Transition-Metal-Mediated Aromatic Ring Construction* (Wiley, Hoboken, 2013)
34. F. Jafarpour, H. Hazrati, Adv. Synth. Catal. **352**, 363 (2010)
35. W. Harris, C.H. Hill, E. Keech, P. Malsher, Tetrahedron Lett. **34**, 8361 (1993)
36. C.B. de Koning, J.P. Michael, A.L. Rousseau, Tetrahedron Lett. **39**, 8725 (1998)
37. Z. Shi, S. Ding, Y. Cui, N. Jiao, Angew. Chem. **121**, 8035 (2009)
38. K. Hirano, Y. Inaba, T. Watanabe, S. Oishi, N. Fujii, H. Ohno, Adv. Synth. Catal. **352**, 368 (2010)
39. X. Cai, V. Snieckus, Org. Lett. **6**, 2293 (2004)
40. J. Yang, Q. Zhang, W. Zhang, W. Yu, RSC Advances **4**, 13704 (2014)
41. E. Kianmehr, M. Ghanbari, N. Faghih, F. Rominger, Tetrahedron Lett. **53**, 1900 (2012)
42. E. Kianmehr, A. Rajabi, M. Ghanbari, Tetrahedron Lett. **50**, 1687 (2009)
43. K. Jadidi, R. Ghahremanzadeh, M. Mehrdad, M. Ghanbari, H. Arvin-Nezhad, Monatsh. Chem. **139**, 277 (2008)
44. E. Kianmehr, N.S. Zafarghandi, M. Ghanbari, Mol. Divers. **17**, 383 (2013)
45. A.S.K. Hashmi, M. Ghanbari, M. Rudolph, F. Rominger, Chem. Eur. J. **18**, 8113 (2012)
46. E. Kianmehr, M. Ghanbari, M.N. Niri, R. Faramarzi, J. Comb. Chem. **12**, 41 (2009)
47. E. Kianmehr, M. Ghanbari, Eur. J. Org. Chem. **2012**, 256 (2012)
48. CCDC-1040369 (8a) contains the supplementary crystallographic data for this paper. These data can be obtained free of charge from The Cambridge Crystallographic Data Centre. www.ccdc.cam.ac.uk/data_request/cif
49. M. Viji, S.K. Ghosh, R. Nagarajan, Synthesis **46**, 955 (2014)
50. B.S. Lane, M.A. Brown, D. Sames, J. Am. Chem. Soc. **127**, 8050 (2005)
51. X. Wang, D.V. Gribkov, D. Sames, J. Org. Chem. **72**, 1476 (2007)
52. D.J. Cárdenas, B. Martín-Matute, A.M. Echavarren, J. Am. Chem. Soc. **128**, 5033 (2006)
53. CCDC-1040370 (11) contains the supplementary crystallographic data for this paper. These data can be obtained free of charge from The Cambridge Crystallographic Data Centre. www.ccdc.cam.ac.uk/data_request/cif
54. S. Fioravanti, L. Pellacani, P.A. Tardella, M.C. Vergari, Org. Lett. **10**, 1449 (2008)
55. A.T.R. William, S.A. Winfield, J.N. Miller, Analyst **108**, 1067 (1983)
56. W. Melhuish, J. Phys. Chem. **65**, 229 (1961)
57. W. Rettig, M. Zander, Chem. Phys. Lett. **87**, 229 (1982)
58. A. Kapturkiewicz, J. Herbich, J. Karpiuk, J. Nowacki, J. Phys. Chem. A **101**(12), 2332–2344 (1997)